ISSN 0097-8078, Water Resources, 2019, Vol. 46, No. 3, pp. 353–366. © Pleiades Publishing, Ltd., 2019.

HYDROPHYSICAL PROCESSES

Turbulence Study Around Bar in a Braided River Model[1]

Md. Amir Khan[a], * and Nayan Sharma[a], **

[a] *Department of Water Resources Development and Management, IIT Roorkee, Roorkee, India*

**e-mail: amirmdamu@gmail.com*

***e-mail: nayanfwt@gmail.com*

Received August 29, 2016; revised August 29, 2016; accepted January 27, 2017

Abstract—Turbulent flow is a flow regime which is described by the anarchic property changes. This includes the rapid variation of pressure, high momentum convection and flow velocity in time and space. A turbulent phenomenon in a braided river is much more complex as compared to the straight and meandering rivers. Turbulent flow characteristics around the braid bar are not thoroughly studied till now. In the current paper, the quadrant method is used to analyze the turbulence characteristics of flow around the island in a braided river model using 2-D burstingevents technique. Three velocity fluctuation components (u', v', w'), were measured with Acoustic Doppler Velocimetry. Although many advances have been made within recent years in interpreting the mechanics of flow, transport of sediment and sedimentary architecture of braided rivers, many key issues remains to be addressed, in particular, the underlying processes of braid bar initiation. An attempt has been made herein to relate the depositional characteristics around the island in the braided river model to the sweep and ejection events. The concept of the hole is used in order to isolate the extreme events that contribute to the turbulent burst. The angle of sweep and ejection events are calculated at points around the island. The angle of events at these points depict the pattern similar to scouring/ deposition at points around the island in the braided river model.

Keywords: acoustic doppler velocimeter, braided bar, turbulence, braided

DOI: 10.1134/S0097807819030023

INTRODUCTION

In the natural condition, there are several river patterns such as a straight river, meandering river, braided river exist. The structure of secondary current, bed shear stress in the meandering channel have been thoroughly studied by conducting experiments and numerical simulation. Some research has been done to understand the turbulence characteristics of flow in braided river, however, these works are not sufficient to fully understand the turbulence characteristics of flow around the braid bar [7, 13, 14]. A turbulent phenomenon in braided rivers is much more complex than that in straight and meandering rivers, since turbulent flow characteristics around the braid bar are not well researched and understood till now [1, 11]. Braiding of the river is characterized by the division of channel around an alluvial island. The growth of the islands gets initiated as the coarser portion of sediment load start depositing. The bar grows downstream and in height due to the continuous deposition of sediment on its surface, diverting the water into the flanking channels, which to carry the flow, deepen and cut laterally into the original banks. Deepening of flanking channel locally lowers the water depth and the bar emerges as an island which becomes stabilized by vegetation [5]. In this study, the model of the braided river is constructed in the lab. The island of size 30 by 45 cm is constructed in the mid portion of the channel. The main purpose of this study is to relate the quadrant bursting events to the erosion and deposition procesess around the braided island.

Braiding and Turbulence

Both turbulence and stream braiding phenomena are represented by a hierarchy of scales. In turbulence the objects constituting these scales are referred as eddies; for braiding, the bar, the term is used analogously for all types of sediment islands, including the whole zoology of bar types described by the previous researchers. Turbulence and braiding both exhibit fractal behavior within the hierarchy of scales [4, 12]. Also, in both types of systems interactions between structures give rise to short-lived events (ejection and sweep in turbulence and confluences in braiding) that contributes disproportionately to the overall net transport (momentum in turbulence; sediment in braiding).

[1] The article is published in the original.

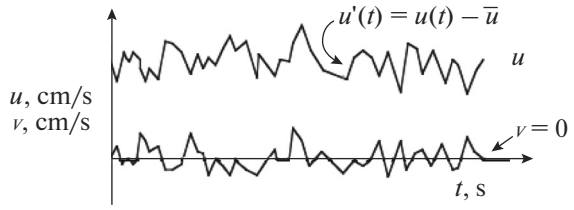

Fig. 1. Recorded velocity distribution for turbulent flow.

Characterizing Turbulence

Turbulent eddies create fluctuations in velocity, these fluctuations represent the chaotic motion. The velocity measured at any point t consists of mean value and turbulence fluctuations,as shown in Eqs. (1) and (2):

$$u'(t) = \bar{u} - u(t), \tag{1}$$

$$v'(t) = \bar{v} - v(t). \tag{2}$$

$\bar{u}$, $\bar{v}$ represents the average velocity in the longitudinal and vertical directions respectively, $u(t)$ and $v(t)$ represent the instantaneous longitudinal and vertical velocity at time t respectively. $u'(t)$ and $v'(t)$ represent the instantaneous turbulent fluctuations in the longitudinal and vertical directions at time t respectively (Fig. 1).

Turbulent flow can be characterized by the statistical concepts, theoretically velocity is assumed continuous and mean velocity is calculated by integration. However, in practice velocity records consist of discrete points $u(t)$, hence mean velocity is calculated by summation of all discrete velocities divided by the number of discrete points as shown in Eqs. (3) and (4).

$$\text{Mean velocity:}\quad \bar{u} = \frac{1}{N}\sum_{I}^{N} u_i, \tag{3}$$

$$\text{Turbulent fluctuation:}\quad u'(t) = u_i' = u_i - \bar{u}, \tag{4}$$

$$\text{Turbulent strength:}\quad u_{rms} = \sqrt{\frac{1}{N}\sum_{i=1}^{N}(u_i')^2}, \tag{5}$$

$$\text{Turbulence intensity:}\quad u_{rms}/\bar{u}. \tag{6}$$

Here, u_i represents the ith discrete velocity components, u_i' represents the fluctuating components of ith velocity sample, $\bar{u}$ represents the mean velocity of the N discrete samples of velocity.

Quadrant Analysis

The conventional quadrant method involves studying the relationship between temporal fluctuations of velocity components, u' and v', particularly their distribution between four quadrants numbered as shown in Fig. 2. Based on quadrant analysis turbulent phenomenon is characterized into the four quadrants

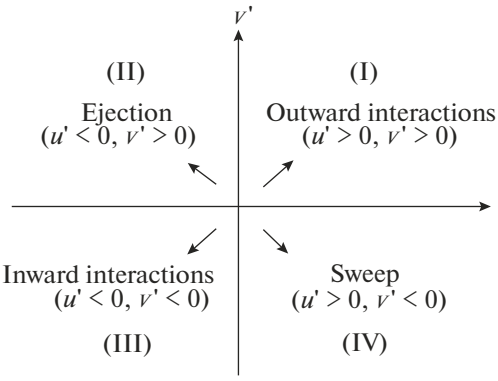

Fig. 2. Four classes of bursting events and the associated quadrant.

depending on the sign of fluctuating velocity u' and v'. First quadrant Outward interaction in which $u_i' > 0$, $v_i' > 0$; Second quadrant Ejection in which $u_i' < 0$, $v_i' > 0$; Third quadrant Inward interaction in which $u_i' < 0$, $v_i' < 0$; Fourth quadrant Sweep in which $u_i' > 0$, $v_i' < 0$.

Out of these four-quadrant events, sweep and ejection are relatively more important and they are related to the sediment entrainment and transport in the river. The contribution of the coherent structure mainly sweep (Quadrant IV) and ejection (Quadrant II) are intensively studied by the several researchers. A.J. Grass and J.M. Nelson et al. [2, 8] have extensively studied quadrant events, and they found that sweep is most important event that is related to transfer of momentum into the boundary layer. In addition, they found that close to bed the frequency of sweep and ejection is more as compared to the outward interaction (Quadrant I) and inward interaction (Quadrant III) events.

Experimental Program

The experiments were conducted in River Engineering Laboratory, Department of Water Resources Development and Management, Indian Institute of Technology Roorkee, India. The experiments were carried out in a flume 2.6 m wide, 1 m deep and 10 m long. Experiments were carried out at three different water flow rate of 0.06, 0.05 and 0.03 m^3/s. The tailgate was used to maintain the flow depth. The slope of the flume is kept constant for all the runs. Velocity is measured at 12 points around the island (as shown in Fig. 3) in a braided river model with the help of ADV. The frequency of occurrence of each quadrant event was calculated at 12 selected points around the island for three different discharges as shown in Figs. 4–6. The velocity was measured at the distance of 0.6 cm from the bed at these points. The objective of this experimental program is to relate the sweep and ejection events to the deposition and erosion pattern around the island in a braided river model. H. Naka-

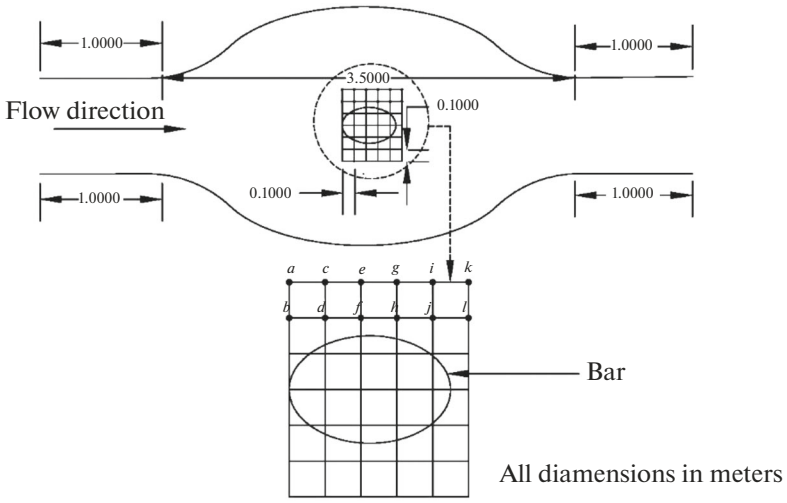

Fig. 3. Sketch of the braided river model.

gwa and I. Nezu [9] found that the sweep event is closely related to the sediment entrainment. The erosion/deposition data are collected around the island at these selected 12 points for three different discharge (Fig. 3). The experiments were carried out at three different discharges. H. Nakagwa and I. Nezu [9] found that only the extreme quadrant events contribute to the burst in turbulent flow, and in order to exclude the extreme events from low-intensity events, different sizes of a hole are defined. The frequency of occurrence of quadrant events for different hole size is plotted for 12 different points around the island. The effect of hole sizes on the frequency of occurrence of each quadrant event is also studied in this paper. The mean angle of sweep and ejection are also plotted at 12 different points around the island. It was found that the mean angle of sweep and ejection events are related to scouring around the island in a braided river model. The detailed information of the experimental study is displayed in Table 1.

DATA ANALYSIS AND RESULTS

I. Nezu [10] found that only extreme events contribute to the Reynold Stress,and the hyperbolic hole is defined in order to isolate the extreme events within each quadrant. The hole is defined by the resulting curves as yielded from Eq. (7):

$$\left|u'(z,t)\,v'(z,t)\right| = q\sqrt{\overline{u'(z,t)^2}}\sqrt{\overline{v'(z,t)^2}}, \tag{7}$$

where q represents the hole size, the over-bar represents the time averaged value, $u'(z, t)$ and $v'(z, t)$ represent the instantaneous longitudinal and vertical turbulent fluctuations respectively. Instantaneous Reynolds Stress for each measuring points has been filtered by applying function $E_k(z, t)$ where k = I, II, III, IV indicates the quadrant where the turbulent event falls. Discriminating function $E_k(z, t)$ has been defined below.

$$\begin{cases} E_{\mathrm{I}}(z,t) = 1, \\ E_{\mathrm{I}}(z,t) = 0, \\ \begin{cases} \text{if } u'(z,t) > 0; \;\; v'(z,t) > 0 \\ \text{excluding hole describe by Eq. (7)} \\ \text{elsewhere,} \end{cases} \end{cases} \tag{8}$$

$$\begin{cases} E_{\mathrm{II}}(z,t) = 1, \\ E_{\mathrm{II}}(z,t) = 0, \\ \begin{cases} \text{if } u'(z,t) < 0; \;\; v'(z,t) > 0 \\ \text{excluding hole describe by Eq. (7)} \\ \text{elsewhere,} \end{cases} \end{cases} \tag{9}$$

Table 1. The details of experimental condition performed in this study

Serial no	Experimental condition code	Condition	Discharge, m^3/s	Depth of flow, cm
1	*W*	No bar	0.06	27
2	*X*	Presence of bar	0.06	27
3	*Y*	Presence of bar	0.05	23
4	*Z*	Presence of bar	0.03	21

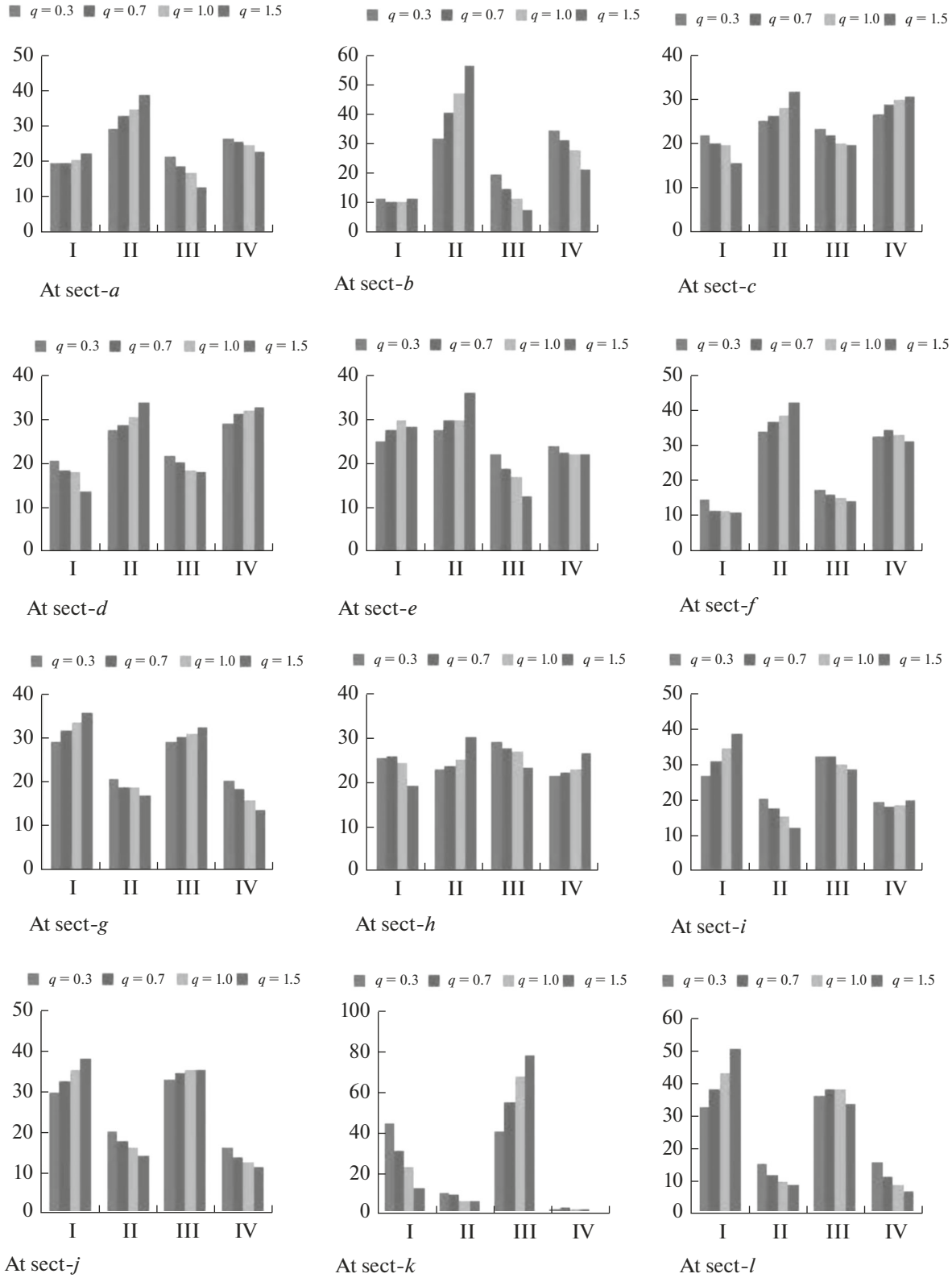

Fig. 4. The histogram of the values of $f_K(z)$ determined at a depth of 0.6 cm from the bed for four different threshold level (q = 0.3, q = 0.7, q = 1.0, q = 1.5) at 12 point near the braided bar (experimental condition *X*).

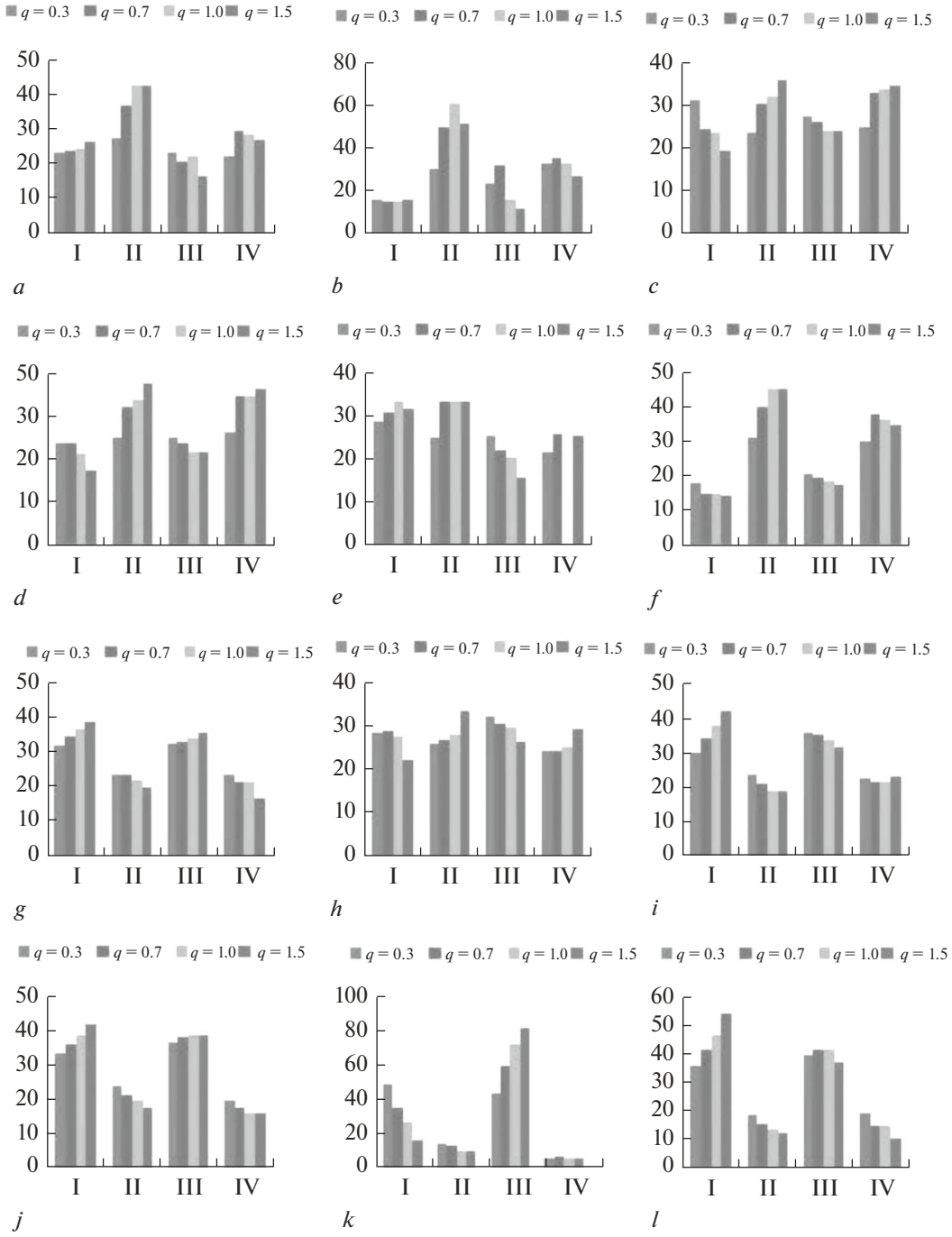

Fig. 5. The histogram of the values of $f_K(z)$ determined at a depth of 0.6 cm from the bed for four different threshold level (q = 0.3, q = 0.7, q = 1.0, q = 1.5) at 12 point near the braided bar (experimental condition *Y*).

$$\begin{cases} E_{\mathrm{III}}(z,t) = 1, \\ E_{\mathrm{III}}(z,t) = 0, \\ \begin{cases} \text{if } u'(z,t) < 0; \quad v'(z,t) < 0 \\ \text{excluding hole describe by Eq. (7)} \\ \text{elsewhere,} \end{cases} \end{cases} \tag{10}$$

$$\begin{cases} E_{\mathrm{IV}}(z,t) = 1, \\ E_{\mathrm{IV}}(z,t) = 0, \\ \begin{cases} \text{if } u'(z,t) > 0; \quad v'(z,t) < 0 \\ \text{excluding hole describe by Eq. (7)} \\ \text{elsewhere.} \end{cases} \end{cases} \tag{11}$$

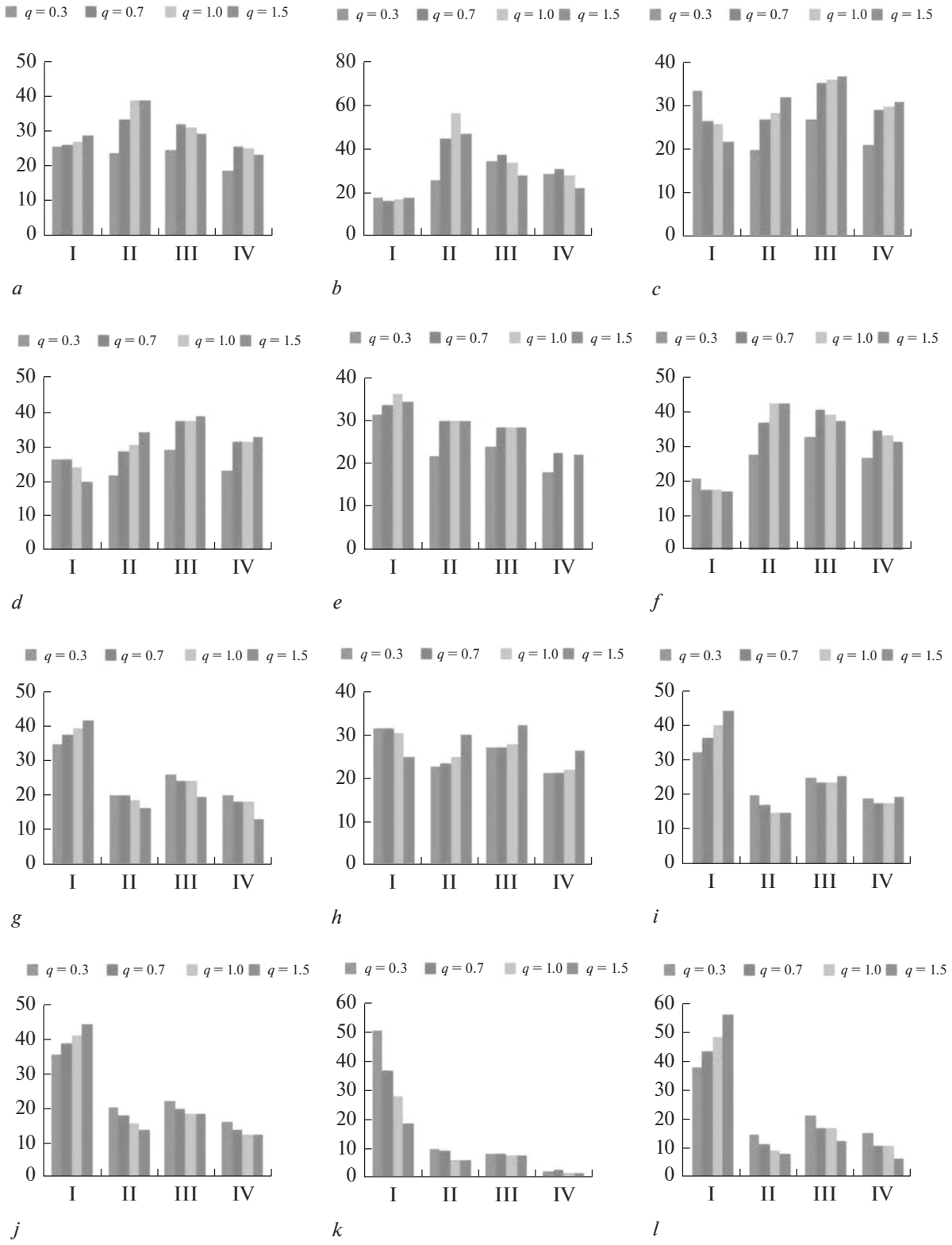

Fig. 6. The histogram of the values of $f_K(z)$ determined at a depth of 0.6 cm from the bed for four different threshold level (q = 0.3, q = 0.7, q = 1.0, q = 1.5) at 12 point near the braided bar (experimental condition *Z*).

The function $E_k(z, t)$ shown in Eqs. (8)–(11) allows recognition of the fluctuating velocity that are contributing to the turbulent events. After excluding the turbulent event that falls in the inside region of the hole, the remaining turbulent event contributes to Reynolds stress. A small value of q leads to the selection of both strong and weak events. For the large value of hole size q only the strong events are considered for the turbulent burst. Percent occurrence of each turbulent event is calculated by Eq. (12) [6, 15]:

$$\left[f_K(z) = \frac{\sum_{t=0}^{T} E_k(z,t)}{\sum_{t=0}^{T} E_{\mathrm{I}}(z,t) + \sum_{t=0}^{T} E_{\mathrm{II}}(z,t) + \sum_{t=0}^{T} E_{\mathrm{III}}(z,t) + \sum_{t=0}^{T} E_{\mathrm{IV}}(z,t)} \right], \quad (12)$$

where $\sum_{t=0}^{T} E_k(z,t)$ is the number of turbulent event occurring in the kth quadrant excluding hole, T is the measurement time length.

The frequency of occurrence of each quadrant event is calculated at 12 nodal points around an island of the height of 14 cm in a braided river model using Eq. (12). The histogram of frequency of occurrence of each quadrant events for different sizes of hole and discharge at 12 nodal points are displayed in Figs. 4–6. The frequency of occurrence of each quadrant events for different hole sizes and discharge rate are displayed in Fig. 7. The frequency of occurrence of quadrant events for the experimental conditions X (Fig. 4), shows that the sweep and ejection are dominant events from point a to point f. The outward interaction and inward interaction are dominant events at the remaining six points. The frequency of occurrence of each quadrant events is plotted for different values of hole size. At point a, the dominant eventsis ejection, frequency of ejection events is around 31% at $q = 0.3$, it is increased to 41% at $q = 1.5$. Similarly, the frequency of occurrence of outward interaction(dominating events) at point g increases from 29.24 at $q = 0.3$ to 36.14 at $q = 1.5$. From above results, it is clearly visible that the frequency of occurrence of the dominant events increases with increase in the size of the hole. The main function of the hole is to filter out the extreme event from the low magnitude event. The hole filtered out the extreme events that are contributing to the burst. After analysis of the frequency of occurrence of each quadrant event, it was found that from point a to point f scouring occurs,and at these points sweep and ejection are dominating events. Deposition occurs at the remaining six points. At these points, outward interaction and inward interaction are dominating events. Thus, it can be concluded that 'sweep' and 'ejection' are related to erosion. Evidently, higher values of sweep and ejection occurrence frequency indicate the erosion, whereas 'outward interaction', and 'inward interaction'are related to deposition around the island in a braided river model.

Table 2 shows the experimental results ofscouring and deposition patterns at 12 points around the island in a braided river model for three different experimental conditions. The bed levels at these points were taken before starting and after completion of the experiments. The differences between the final bed level after the completion of experiments and the initial bed level were calculated, wherein negative values of difference represent the erosion and positive values represent the deposition at that points.

Experiments were performed at three different discharge values. For the hole size of 0.3, the frequency of occurrence of the sweep events at point a decreases from 30.15 to 27.15 when the discharge decreases from 0.06 to 0.05 cm^3/s, the frequency of occurrence of sweep events is further decreased to 24.15 at the discharge of 0.03 cm^3/s (Tables 3–5). The frequency of occurrence of ejection events shows the similar trend with the discharge. Remaining 11 points also shows the similar decrease in frequency of occurrence of sweep and ejection events with a decrease in the value of discharge. As stated earlier above, scouring and deposition pattern around an island in a braided river model is presented in Table 2, which shows that the deposition occurs at the points g, h, i, j, k, l, and the deposition at these points increases with the decrease in discharge. So from the above results, it can be concluded that the frequency of occurrence of sweep and ejection decreases and deposition around the island increases with a decrease in the discharge. The above

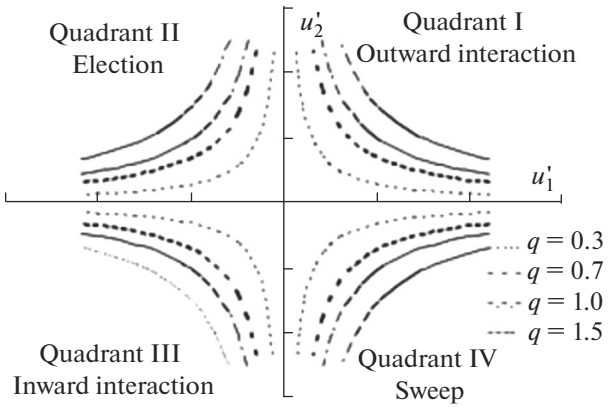

Fig. 7. The quadrant event for different hole.

Table 2. The model experimental results of the scouring and deposition patterns at different positions around bar

Point	Experiment *W* erosion/deposition, cm	Experiment *X* erosion/deposition, cm	Experiment *Y* erosion/deposition, cm	Experiment *Z* erosion/deposition, cm
a	−1.1	−4.32	−3.42	−3.12
b	−0.91	−5.12	−4.22	−3.92
c	−0.75	−3.45	−2.55	−2.25
d	−0.82	−4.28	−2.88	−2.58
e	−0.78	−1.9	−1.6	−1.3
f	−1.21	−1.2	−1.42	−1.12
g	−1.32	0.2	0.6	1
h	−0.94	0.4	0.8	1.2
i	−0.78	0.5	0.9	1.1
j	−0.88	0.8	1.1	1.5
k	−1.12	0.9	1.2	1.6
l	−1.13	1.1	1.5	1.9

Table 3. The frequency of occurrence of the quadrant events for different sizes of hole at 12 different points around the braided island for experimental condition *X*

Experimental condition *X*												
For $q = 0.3$ Frequency of occurrence												
events	point *a*	point *b*	point *c*	point *d*	point *e*	point *f*	point *g*	point *h*	point *i*	point *j*	point *k*	point *l*
Quadrant 1	20.17	12.37	27.76	20.75	25.47	15.15	29.24	25.78	26.98	29.90	45.16	32.59
Quadrant 2	30.15	32.35	26.05	28.05	27.84	34.21	20.83	23.27	20.77	20.77	10.55	15.52
Quadrant 3	20.12	20.12	23.94	21.94	22.31	17.75	29.38	29.36	32.53	33.22	40.56	36.04
Quadrant 4	25.14	35.14	27.24	29.29	24.36	32.86	20.54	21.57	19.71	16.58	2.70	15.83
For $q = 7$ Frequency of occurrence												
Quadrant 1	20.48	10.99	20.88	20.75	27.89	11.86	31.96	25.99	31.22	32.89	31.54	38.08
Quadrant 2	33.83	45.51	27.10	29.10	30.27	37.07	20.82	23.80	17.87	18.12	9.93	12.12
Quadrant 3	17.48	28.12	22.54	20.54	19.06	16.31	30.29	27.88	32.42	34.85	55.48	38.33
Quadrant 4	26.36	31.83	29.46	31.46	22.76	34.75	18.65	21.57	18.47	14.12	3.05	11.45
For $q = 1$ Frequency of occurrence												
Quadrant 1	21.38	11.25	20.22	18.22	30.24	11.89	33.74	24.74	34.90	35.43	22.89	42.89
Quadrant 2	39.46	57.20	28.77	30.77	30.14	42.46	19.22	25.18	15.77	16.23	6.70	9.97
Quadrant 3	19.32	12.26	20.62	18.62	17.13	15.27	31.04	27.09	30.43	35.68	68.08	38.15
Quadrant 4	25.66	28.69	30.26	31.46	22.47	33.55	18.65	22.31	18.47	12.63	2.31	11.45
For $q = 1.5$ Frequency of occurrence												
Quadrant 1	23.24	12.28	16.11	14.11	28.63	11.30	36.14	19.38	38.88	38.47	13.12	50.43
Quadrant 2	39.46	47.78	32.30	34.30	30.14	42.46	17.10	30.58	15.77	14.34	6.71	8.87
Quadrant 3	13.55	8.26	20.49	18.49	12.73	14.57	32.77	23.42	28.70	35.43	78.49	33.54
Quadrant 4	23.72	22.74	31.09	33.09	22.45	31.65	13.97	26.61	20.13	12.63	2.17	7.14

Table 4. The frequency of occurrence of the quadrant events for different sizes of hole at 12 different points around the braided island for experimental condition *Y*

Experiment condition *Y*												
For $q = 0.3$ Frequency of occurrence												
events	point *a*	point *b*	point *c*	point *d*	point *e*	point *f*	point *g*	point *h*	point *i*	point *j*	point *k*	point *l*
Quadrant 1	23.17	15.37	30.76	23.75	28.47	18.15	32.24	28.78	29.98	32.9	48.16	35.59
Quadrant 2	27.15	29.35	23.05	25.05	24.84	31.21	23.83	26.27	23.77	23.77	13.55	18.52
Quadrant 3	23.12	23.12	26.94	24.94	25.31	20.75	32.38	32.36	35.53	36.22	43.56	39.04
Quadrant 4	22.14	32.14	24.24	26.29	21.36	29.86	23.54	24.57	22.71	19.58	5.7	18.83
For $q = 7$ Frequency of occurrence												
Quadrant 1	23.48	13.99	23.88	23.75	30.89	14.86	34.96	28.99	34.22	35.89	34.54	41.08
Quadrant 2	36.83	48.51	30.1	32.1	33.27	40.07	23.82	26.8	20.87	21.12	12.93	15.12
Quadrant 3	20.48	31.12	25.54	23.54	22.06	19.31	33.29	30.88	35.42	37.85	58.48	41.33
Quadrant 4	29.36	34.83	32.46	34.46	25.76	37.75	21.65	24.57	21.47	17.12	6.05	14.45
For $q = 1$ Frequency of occurrence												
Quadrant 1	24.38	14.25	23.22	21.22	33.24	14.89	36.74	27.74	37.9	38.43	25.89	45.89
Quadrant 2	42.46	60.2	31.77	33.77	33.14	45.46	22.22	28.18	18.77	19.23	9.7	12.97
Quadrant 3	22.32	15.26	23.62	21.62	20.13	18.27	34.04	30.09	33.43	38.68	71.08	41.15
Quadrant 4	28.66	31.69	33.26	34.46	25.47	36.55	21.65	25.31	21.47	15.63	5.31	14.45
For $q = 1.5$ Frequency of occurrence												
Quadrant 1	26.24	15.28	19.11	17.11	31.63	14.3	39.14	22.38	41.88	41.47	16.12	53.43
Quadrant 2	42.46	50.78	35.3	37.3	33.14	45.46	20.1	33.58	18.77	17.34	9.71	11.87
Quadrant 3	16.55	11.26	23.49	21.49	15.73	17.57	35.77	26.42	31.7	38.43	81.49	36.54
Quadrant 4	26.72	25.74	34.09	36.09	25.45	34.65	16.97	29.61	23.13	15.63	5.17	10.14

observations show that the frequency of occurrence of sweep and ejection events are inversely related to deposition around the island in the braided river model.

Probability of Occurrence of Coherent Flow and Bursting Events

Based on two dimensional velocity fluctuations, the probability of the occurrence of each quadrant bursting events is determined by Eq. (13) [3]:

$$P_k = \frac{n_k}{N}, \tag{13}$$

$$N = \sum_{k=1}^{4} n_k, \tag{14}$$

where P_k is the probability of occurrence of the events belonging to quadrant k, n_k is the number of events belonging to k quadrant, N is total number of velocity samples. Using the equation given above, the probability of occurrence of sweep and ejection quadrant events was calculated at given point of flow within the depth. The contributions of the sweep (Quadrant IV) and ejection (Quadrant II) events to momentum transfer have been thoroughly studied by using quadrant technique and probability analysis. The conditional probability of occurrence of sweep and ejection quadrant events is calculated at twelve different points at the distance of 0.6 m from the bed. The conditional probability of sweep and ejection events along with the deposition/scouring pattern at 12 points around the island for three different experimental conditions are displayed in Fig. 8.

As already mentioned earlier, Table 2 indicates erosion and deposition pattern around the island in the braided river model, negative values indicate erosion and positive values indicate deposition. From Fig. 8 it is indicated that the conditional probability of sweep and ejection events is in phase with the erosion and deposition pattern around the island in the braided river model at 12 measured points. The values of conditional probability of sweep and ejection events are high at points of erosion and their values are low at the points of deposition. This shows that the sweep and ejection events are related to the erosion around the bar. However, a large amount of experiment is required to validate relation between sweep and ejection events to erosion and deposition around the island in a braided river model.

For all the three discharges, the conditional probability of sweep and ejection events computed at 12 dif-

Table 5. The frequency of occurrence of the quadrant events for different sizes of hole at 12 different points around the braided island for experimental condition *Z*

Experimental condition *Z*												
For $q = 0.3$ Frequency of occurrence												
events	point *a*	point *b*	point *c*	point *d*	point *e*	point *f*	point *g*	point *h*	point *i*	point *j*	point *k*	point *l*
Quadrant 1	26.17	18.37	33.76	26.75	31.47	21.15	35.24	31.78	32.98	35.9	51.16	38.59
Quadrant 2	24.15	26.35	20.05	22.05	21.84	28.21	20.83	23.27	20.77	20.77	10.55	15.52
Quadrant 3	25.14	35.14	27.24	29.29	24.36	32.86	26.54	27.57	25.71	22.58	8.7	21.83
Quadrant 4	19.14	29.14	21.24	23.29	18.36	26.86	20.54	21.57	19.71	16.58	2.7	15.83
For $q = 0.7$ Frequency of occurrence												
Quadrant 1	26.48	16.99	26.88	26.75	33.89	17.86	37.96	31.99	37.22	38.89	37.54	44.08
Quadrant 2	33.83	45.51	27.1	29.1	30.27	37.07	20.82	23.8	17.87	18.12	9.93	12.12
Quadrant 3	32.36	37.83	35.46	37.46	28.76	40.75	24.65	27.57	24.47	20.12	9.05	17.45
Quadrant 4	26.36	31.83	29.46	31.46	22.76	34.75	18.65	21.57	18.47	14.12	3.05	11.45
For $q = 1$ Frequency of occurrence												
Quadrant 1	27.38	17.25	26.22	24.22	36.24	17.89	39.74	30.74	40.9	41.43	28.89	48.89
Quadrant 2	39.46	57.2	28.77	30.77	30.14	42.46	19.22	25.18	15.77	16.23	6.7	9.97
Quadrant 3	31.66	34.69	36.26	37.46	28.47	39.55	24.65	28.31	24.47	18.63	8.31	17.45
Quadrant 4	25.66	28.69	30.26	31.46	22.47	33.55	18.65	22.31	18.47	12.63	2.31	11.45
For $q = 1.5$ Frequency of occurrence												
Quadrant 1	29.24	18.28	22.11	20.11	34.63	17.3	42.14	25.38	44.88	44.47	19.12	56.43
Quadrant 2	39.46	47.78	32.3	34.3	30.14	42.46	17.1	30.58	15.77	14.34	6.71	8.87
Quadrant 3	29.72	28.74	37.09	39.09	28.45	37.65	19.97	32.61	26.13	18.63	8.17	13.14
Quadrant 4	23.72	22.74	31.09	33.09	22.45	31.65	13.97	26.61	20.13	12.63	2.17	7.14

Table 6. The conditional probability of the sweep and ejection events at 12 different points around the island for three experimental conditions

Experiment *X*	Conditional probability, %											
events	point *a*	point *b*	point *c*	point *d*	point *e*	point *f*	point *g*	point *h*	point *i*	point *j*	point *k*	point *l*
2	0.33	0.35	0.29	0.31	0.3	0.37	0.23	0.26	0.23	0.23	0.13	0.18
4	0.28	0.38	0.3	0.32	0.27	0.35	0.23	0.24	0.22	0.19	0.05	0.18
Experiment *Y*	Conditional probability											
2	0.25	0.35	0.27	0.29	0.24	0.32	0.25	0.28	0.25	0.25	0.15	0.2
4	0.3	0.32	0.26	0.28	0.27	0.34	0.25	0.26	0.24	0.21	0.15	0.2
Experiment *Z*	Conditional probability											
2	0.23	0.33	0.25	0.27	0.22	0.3	0.23	0.26	0.23	0.23	0.13	0.18
4	0.28	0.3	0.24	0.26	0.25	0.32	0.23	0.24	0.22	0.19	0.13	0.17

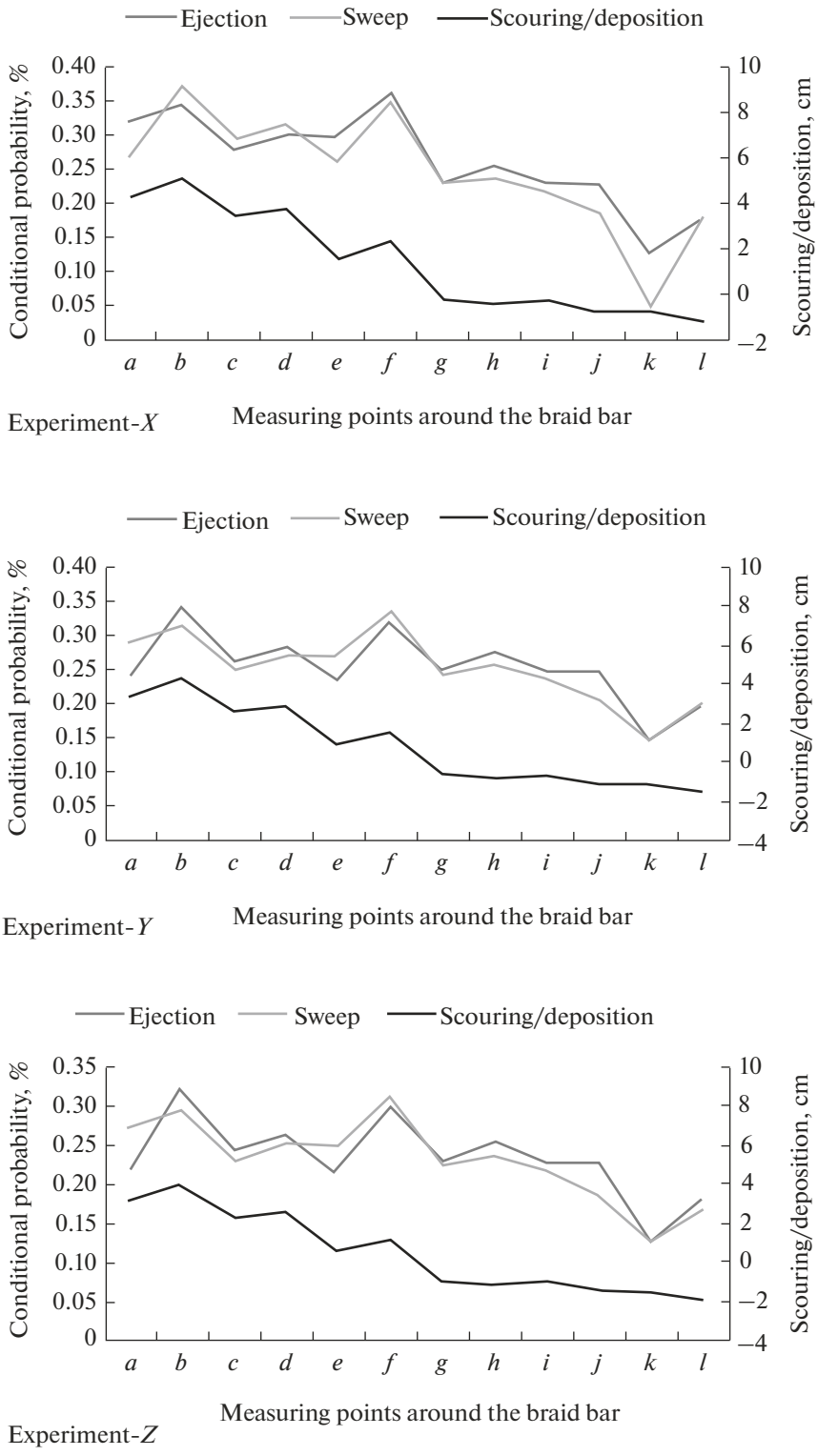

Fig. 8. The conditional probability and scouring/deposition pattern plotted at 12 points around the island in a braided river model for three different experimental conditions.

ferent points are in phase with the erosion and deposition around the island in a braided river model as shown in Fig. 8. Referring to Table 6, at points *a*, the conditional probability of sweep and ejection events are 0.27, 0.32 respectively, and these sweep and ejection events decreases to 0.22, 0.27 respectively when

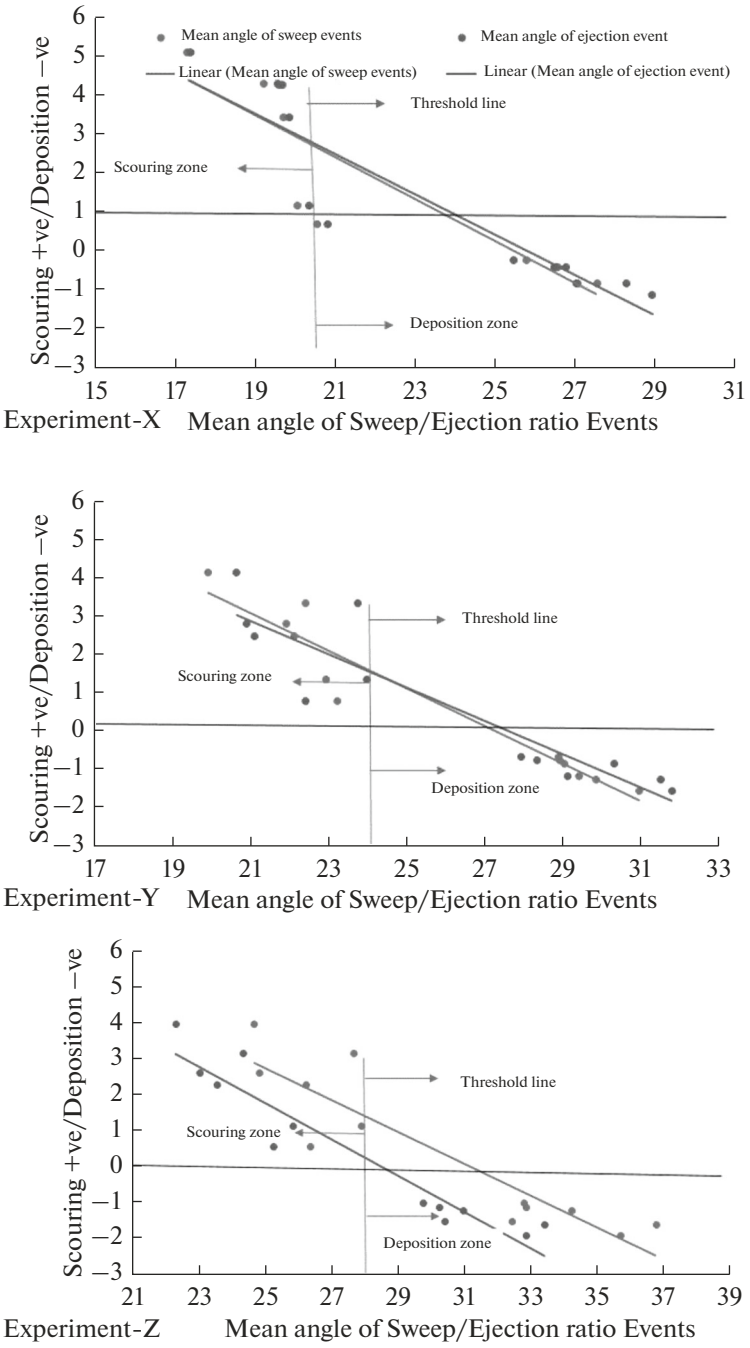

Fig. 9. The angle of sweep and ejection events and scouring/deposition pattern plotted at 12 points around the island in a braided river model for three different experimental conditions.

the discharge decrease from 0.06 to 0.03 m^3/s (Table 6). A similar decrease in sweep and ejection events with a decrease in discharge occurs for remaining 11 points. Scouring and deposition patterns around the island in the braided river model are displayed in Table 2, which shows that the deposition occurs at the points *g*, *h*, *i*, *j*, *k*, *l* and the deposition at these points increases with the decrease in discharge. This shows that the values of the conditional probability of sweep and ejection events are inversely related with the deposition around the island, thus, the low values of sweep events are related to the deposition around the island in the braided river model.

The Angle of the Events

The applied force on the bed particles depends on the inclination angle of the force. The angle of a par-

Table 7. The mean angle of sweep and ejection events at 12 different points around the island for three experimental conditions

Points	Experiment *X*		Experiment *Y*		Experiment *Z*	
	mean sweep angle, °	mean ejection angle, °	mean sweep angle, °	mean ejection angle, °	mean sweep angle, °	mean ejection angle, °
a	19.30	19.65	22.4	23.72	27.72	24.4
b	17.39	17.46	19.9	20.64	24.71	22.36
c	19.78	19.94	22.1	21.1	26.3	23.6
d	19.68	19.76	21.9	20.9	24.9	23.1
e	20.63	20.89	23.2	22.41	26.41	25.3
f	20.13	20.42	22.92	23.95	27.95	25.91
g	25.86	25.54	28.86	27.91	32.86	29.81
h	26.65	26.84	29.01	30.3	34.3	31.01
i	26.61	26.56	28.91	28.31	32.91	30.31
j	27.14	27.1	29.4	29.1	32.49	30.47
k	27.62	28.36	29.82	31.48	36.82	33.47
l	28.43	28.99	30.93	31.76	35.76	32.91

ticular event is defined as the angle of turbulent velocity vector with respect to the longitudinal axis. The angle of an event is determinedusing Eq. (15).

$$\theta_{\text{sweep}} = \arctan\left(\left|\frac{v'_{\text{sweep}}}{u'_{\text{sweep}}}\right|\right),$$
$$\theta_{\text{ejection}} = \arctan\left(\left|\frac{v'_{\text{ejection}}}{u'_{\text{ejection}}}\right|\right), \quad (15)$$

where $\theta_{\text{sweep}}, \theta_{\text{ejection}}$ are the angle of sweep and ejection events measured from the horizontal axis.

The magnitude of the mean angle of events for sweep and ejection events are different and it is not acceptable. In order to compute the mean values of sweep and ejection events, the data are transformed into normal distribution using the Box–Cox power transformation.

The values of the mean angle for sweep and ejection events can be computed by averaging the temporal values of sweep and ejection angle. However, the temporal values of sweep and ejection events are not uniformly distributed andthus their mean values donot represent the actual mean sweep and ejection angle. In order to compute the actual mean values of sweep and ejection events, the data are transformed into normal distribution using the Box–Cox power transformation. A Box–Cox power transformation transformed the original data θ_i to the transformed data denoted by $B(\theta_i)$. Here θ_i represents the temporal values of angle of events of *i*th quadrants, for ejection events $i = 2$ and $i = 4$ for sweep events.

A Box–Cox power transformation is defined, for non-zero values of λ by

$$B(\theta_i) = \frac{(\theta_i + k)^{\lambda} - 1}{\lambda}, \quad (16)$$

and, for zero value of λ, by

$$B(\theta_i) = \ln(\theta_i + k). \quad (17)$$

In the above equations, k is a constant and λ is transformation power. If all the values of angle of events θ are greater than zero then the value of constant k is taken as zero. Box–Cox transformation is applied to a dataset which comprises Quadrant IV events (sweep events) and Quadrant II events (ejection events). The inverse transformation B^{-1} of $B(\theta_i)$ for this situation is given by

$$\theta = [\lambda B(\theta_i) + 1]^{\frac{1}{\lambda}}. \quad (18)$$

The mean values of transformed angle of events for sweep and ejection quadrants were calculated using Eq. (19).

$$\left(\overline{B(\theta)_i} = \frac{1}{n}\sum_{i=1}^{n} B(\theta_i)\right)_{i=2,4}. \quad (19)$$

The inverse Box–Cox transformation was applied to these mean values of sweep and ejection events to enable determination of the mean angle of sweep and ejection events.

The velocity was measured at 0.6 cm from the bed at 12 different points. The mean angle for sweep and ejection events for 12 different points and for three discharges are displayed in Table 7. Figure 9 shows the relationships of mean angle of sweep, ejection events with the erosion/deposition magnitude at points around the island for three different experimental conditions. Threshold lines is also displayed in Fig. 9, the values of mean angle of sweep and ejection events

above the threshold value lies under the deposition zone and vice versa. The abovediscussionshows that the mean angle of sweep and ejection events are strongly related with the erosion/deposition magnitude around the island in a braided river model. The values of threshold are 20.5, 24, 28 degree for experimental conditions *X*, *Y*, *Z* respectively, the value of threshold increases with decrease in discharge values. At point *a*, the value of an angle of sweep events increases from 19.3 to 22.4 when the discharge decreases from 0.06 to 0.05 m^3/s (Table 7). A similar increase in angle of sweep and ejection event occurs for remaining 11 points. For the discharge of 0.03 m^3/s, the magnitude of deposition at point *l* is 1.9 cm, the value of deposition at the same point for the discharge of 0.06 m^3/s is about 1.1. Thus, the magnitude of deposition at point *l* increases with the decrease in the discharge, similar deposition trend with decreasing discharge occurs at *j*, *h*, *i*, *j*, *k* points.

CONCLUSIONS

(1) The experimental results show that the frequency of occurrence of the sweep and ejection events are related to erosion around the island in the braided river model. The higher value of sweep and ejection occurrence frequency indicate erosion and the frequency of occurrence of the outward interaction and inward interaction are related to the deposition around the island in a braided river model. After studying the histogram of quadrant analysis, it was found that dominating quadrant events become more dominant at a higher value of hole size. The frequency of occurrence of sweep and ejection events at points around the island decreases with decrease in the discharge.

(2) From the experimental results, it is indicated that the conditional probability of sweep and ejection events is in phase with the erosion and deposition pattern around the island in the braided river model at 12 measured points. The conditional probability of sweep and ejection events ishigh at points of erosion and their values are low at the points of deposition. This shows that the sweep and ejection are related to the erosion and deposition around the bar. The present experimental results show that the values of the conditional probability of sweep and ejection events decrease, when the discharge decreases. The results also show that the deposition around the bar increases with a decrease in discharge, thus the low values of sweep and ejection events are related with deposition around the island in a braided river model.

(3) Threshold value of mean angle of sweep, ejection arecomputed for three different experimental conditions , the values of mean angle of sweep and ejection events above the threshold value lies under the deposition zone and vice versa. The above discussion shows that the mean angle of sweep and ejection events are strongly related with the erosion/deposition magnitude around the island in a braided river model. The threshold value of sweep, ejection events decreases with increase in discharge.

REFERENCES

1. Ferguson, R.I., *Understanding braiding processes in gravel-bed rivers: progress and unresolved problems*, 1993.
2. Grass, A.J., Structural features of turbulent flow over smooth and rough boundaries, *J. Fluid Mech.*, 1971, vol. 50, pp. 233–255.
3. Keshavarzy, A. and Ball, J., An analysis of the characteristics of rough bed turbulent shear stresses in an open channel, Stochastic Hydro, *Hydraulics*, 1997, vol. 11, no. 3, pp. 193–210.
4. Koziol, A., Scales of turbulent eddies in a compound channel, *Acta Geoph.*, 2014. doi 10.2478/s11600-014-0247-0
5. Leopold, L.B. and Wolman, M.G., River channel patterns: braided, meandering and straight, *USGS Professional Paper*, 1957, vol. 282-B, pp. 39–103.
6. Lu, S.S. and Willmarth, W.W., Measurements of the structure of the Reynolds stress in a turbulent layers, *J. Fluid Mech.*, 1973, vol. 60, pp. 481–511.
7. Murray, A.B. and Paola, C., A cellular model of braided streams, *Nature*, 1994, vol. 371, pp. 54–57.
8. Nelson, J.M., Shreve, R.L., Mclean, S., and Drake, T.G., Role of near-bed turbulence structure in bed load transport and bed form mechanics, *Water Resour. Res.*, 1995, vol. 31, no. 5, pp. 2071–2086.
9. Nakagwa, H. and Nezu, I., Bursting phenomenon near the wall in open channel flow and its simple mathematical model, *Fac Eng Kyoto Univ.*, Japan XL, 1978, vol. 40, pp. 213–240.
10. Nezu, I., *Turbulence in Open-Channel Flows*, 1993.
11. Parker, G., On the cause and characteristic scales of meandering and braiding in rivers, *J. Fluid Mech.*, 1976, vol. 76, no. 3, pp. 457–480.
12. Berge, P., Pomeau, Y. and Vidal, C., *Order Within Chaos*, Paris: Wiley, 1984.
13. Richardson, W.R. and Thorne, C.R., Multiple thread flow and channel bifurcation in a braided river: Brahmaputra-Jamuna River, Bangladesh, *Geomorphology*, 2001, vol. 38, pp. 185–196.
14. Roy and Bergeron, Flow and particle paths at a natural river confluence with coarse bed material, *Geomorphology*, 1990, vol. 3, pp. 99–112.
15. Termini, D. and Sammartano, V., Experimental analysis of relation between coherent turbulent structures and bed forms formation, *Archives of Hydro-Engineering Environ. Mechanics*, 2008, vol. 55, nos. 3–4, pp. 125–143.